### Title

Temporal Profiling of Epitranscriptomic Modulators during Osteogenic Differentiation of Human Embryonic Stem Cells.




### Journal

Journal of Proteome Research, 22(7)



### Authors

Yin, Jiekai

Qi, Tianyu

Yang, Yen-Yu

et al.



### Publication Date

2023-07-07

### DOI

10.1021/acs.jproteome.3c00215

Peer reviewed

HHS Public Access

Author manuscript

*J Proteome Res*. Author manuscript; available in PMC 2024 July 07.

Published in final edited form as:

*J Proteome Res*. 2023 July 07; 22(7): 2179–2185. doi:10.1021/acs.jproteome.3c00215.

# Temporal Profiling of Epitranscriptomic Modulators during Osteogenic Differentiation of Human Embryonic Stem Cells

**Jiekai Yin**,
Environmental Toxicology Graduate Program, University of California Riverside, Riverside, California 92521-0403, United States

**Tianyu F. Qi**,
Environmental Toxicology Graduate Program, University of California Riverside, Riverside, California 92521-0403, United States

**Yen-Yu Yang**,
Department of Chemistry, University of California Riverside, Riverside, California 92521-0403, United States

**Madeline Vera-Colón**,
Environmental Toxicology Graduate Program, University of California Riverside, Riverside, California 92521-0403, United States

**Nicole I. zur Nieden**,
Environmental Toxicology Graduate Program, University of California Riverside, Riverside, California 92521-0403, United States

Department of Molecular, Cell, and Systems Biology, University of California, Riverside, California 92521-0403, United States

**Yinsheng Wang**
Environmental Toxicology Graduate Program, University of California Riverside, Riverside, California 92521-0403, United States

Department of Chemistry, University of California Riverside, Riverside, California 92521-0403, United States

## Abstract

Corresponding Author Phone: (951) 827-2700; yinsheng@ucr.edu.

ASSOCIATED CONTENT

Supporting Information

The Supporting Information is available free of charge at https://pubs.acs.org/doi/10.1021/acs.jproteome.3c00215.

Supplementary experimental section; Figure S1, LC-PRM quantification results; Figure S2, GO analysis of the down-regulated RWE proteins in Group 1; Figure S3, Quantification results of methyltransferases and pseudouridine synthases; Figure S4, PPI network analysis of the down-regulated RWE proteins; Figure S5, Western blot validation of quantification results for METTL1; Figure S6, GSEA enrichment plots; Figure S7, Uncropped Western blot images; Table S2, Top 3 functionally enriched terms of each MCODE complex (PDF)

Table S1, LC-PRM quantification results of epitranscriptomic RWE proteins during the osteogenesis of human embryonic stem cells (XLSX)

Complete contact information is available at: https://pubs.acs.org/10.1021/acs.jproteome.3c00215

The authors declare no competing financial interest.

Osteogenesis is modulated by multiple regulatory networks. Recent studies showed that RNA modifications and their reader, writer, and eraser (RWE) proteins are involved in regulating various biological processes. Few studies, however, were conducted to investigate the functions of RNA modifications and their RWE proteins in osteogenesis. By using LC-MS/MS in parallel-reaction monitoring (PRM) mode, we performed a comprehensive quantitative assessment of 154 epitranscriptomic RWE proteins throughout the entire time course of osteogenic differentiation in H9 human embryonic stem cells (ESCs). We found that approximately half of the 127 detected RWE proteins were down-regulated during osteogenic differentiation, and they included mainly proteins involved in RNA methylation and pseudouridylation. Protein–protein interaction (PPI) network analysis unveiled significant associations between the down-regulated epitranscriptomic RWE proteins and osteogenesis-related proteins. Gene set enrichment analysis (GSEA) of publicly available RNA-seq data obtained from osteogenesis imperfecta patients suggested a potential role of METTL1 in osteogenesis through the cytokine network. Together, this is the first targeted profiling of epitranscriptomic RWE proteins during osteogenic differentiation of human ESCs, and our work unveiled potential regulatory roles of these proteins in osteogenesis. LC-MS/MS data were deposited on ProteomeXchange (PXD039249).

## Graphical Abstract

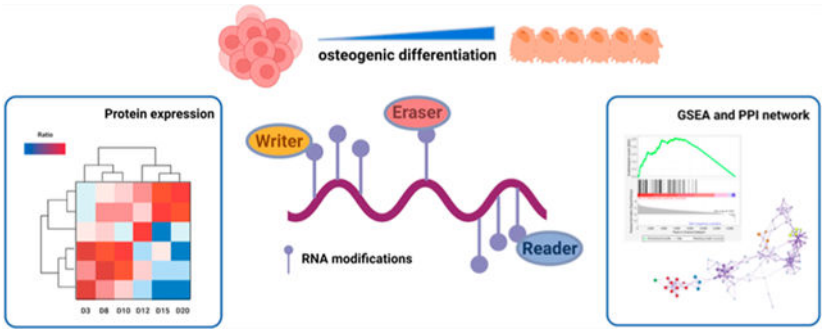


### Keywords

targeted proteomics; parallel-reaction monitoring; osteogenesis; epitranscriptomics; RNA modifications; stem cells; differentiation

## INTRODUCTION

Osteogenesis, i.e., the process of bone formation, usually begins at about six weeks after conception and continues into early adulthood, where growth in bone length stops at around age 25.[1] However, in response to fractures or stress from accidents or physical activities, bone development continues throughout adulthood to repair damage or increase bone thickness for meeting physiological needs. Each year millions of individuals suffer from osteo-degenerative diseases, including osteopenia, osteoporosis, Paget's disease, and osteogenesis imperfecta (OI).[2,3]

Existing treatments for most bone diseases involve two strategies, namely, reducing bone reabsorption and promoting bone formation.[4–6] These treatments, however, only relieve

symptoms and do not cure the diseases, not to mention that there are no effective treatments in some cases.[7] As an emerging therapeutic approach, stem cell therapy has been employed for treating neurodegenerative disorders, ocular disease, diabetes, ischemic heart disease, etc.[8–10] Considering their ability to regenerate bone, stem cells are also used in clinical trials for the treatment of osteoporosis and OI.[11,12] In this vein, embryonic stem cells (ESCs), owing to their immortality and pluripotency, are strong candidates in stem cell therapies for bone diseases.[13]

Osteogenesis is regulated by a sophisticated, multilayered network, which involves various epigenetic and epitranscriptomic mechanisms.[14,15] In the latter respect, epitranscriptomic RNA modifications assume important roles in regulating numerous biological processes.[16] So far, more than 150 modified ribonucleosides have been detected in RNA.[17] Among them, $N^6$-methyladenosine ($m^6A$) stands as the most prevalent internal modification found within mRNAs. Multiple lines of evidence support that $m^6A$, together with its reader, writer, and eraser (RWE) proteins, coordinates with other proteins to regulate osteogenesis.[15] For instance, the $m^6A$ reader protein YTHDF1 regulates zinc-finger protein 839 (ZNF839) in an $m^6A$-dependent manner, where the interaction between ZNF839 and Runx2, a master transcription factor of osteogenic differentiation, promotes the osteogenesis of human bone marrow mesenchymal stem cells (BMSCs).[18] In addition, loss of METTL3, the catalytic subunit of the main $m^6A$ methyltransferase complex, suppressed the osteogenic differentiation of BMSCs.[19] Moreover, FTO, an $m^6A$ demethylase and a component of the GDF11–FTO–PPAR$\gamma$ signaling axis, exhibits a regulatory role in cell fate decision of BMSCs.[20] We reason that, aside from $m^6A$, other modified nucleosides in RNA and their RWE proteins may also regulate osteogenesis.

Here, we induced osteogenic differentiation of H9 human ESCs and performed temporal profiling of epitranscriptomic RWE proteins during the entire time course of osteogenesis. Our results yielded new knowledge about the functions of epitranscriptomic RWE proteins in osteogenesis and advanced the understanding of the complex regulatory networks governing osteogenesis.

## EXPERIMENTAL SECTION

### Cell Culture and Osteogenic Differentiation

H9 Human embryonic stem cells (WiCell) were cultured with mTeSR plus medium (Stem Cell Technologies) on a Matrigel (BD Bioscience)-coated surface, as described recently.[21] The initiation of differentiation followed previously established protocols.[21–24] In brief, ESCs were withdrawn from pluripotency by culturing in Dulbecco's Modified Medium (DMEM, Gibco) supplemented with 15% fetal bovine serum (Atlanta Biologicals), 0.5% penicillin–streptomycin (Gibco), 0.1 mM $\beta$-mercaptoethanol (Sigma), and 1% nonessential amino acids (Gibco) for 5 days. The cells were subsequently cultured in the same medium but supplemented with 50 $\mu$g/mL sodium ascorbate (Sigma), 10 mM $\beta$-glycerophosphate, and 0.12 $\mu$M vitamin D3 for an additional 15 days to further induce osteogenesis. Under these conditions, the cells were differentiated into osteoprogenitor cells at around day 10 postinduction and fully differentiated into mature osteoblasts at days 15–20, as confirmed by Western blot analysis of an osteogenesis marker (i.e., OCN) and calcification

measurement.[21] Confluent cells prior to differentiation induction were collected as Day-0, and the cells after differentiation/osteogenesis induction were collected as indicated.

### LC-PRM Analysis

LC-PRM analyses of 154 epitranscriptomic RWE proteins were conducted on a Q Exactive Plus quadrupole-Orbitrap mass spectrometer equipped with a Nanospray Flex ionization source and coupled to a Dionex UltiMate 3000 RSLCnano UPLC system. The peptide mixture was first loaded and trapped on a home-packed column (150 $\mu$m ID × 40 mm) with 5 $\mu$m Reprosil-Pur C18-AQ resin (Dr. Maisch GmbH HPLC), at a flow rate of 2 $\mu$L/min within 8 min. The peptides were then eluted onto an analytical column (75 $\mu$m ID × 200 mm) packed in-house with 3 $\mu$m Reprosil-Pur C18-AQ resin (Dr. Maisch GmbH HPLC), at a flow rate of 300 nL/min. Formic acid (0.1%, v/v) in water and in acetonitrile/$H_2O$ (80:20, v/v) were used as mobile phases A and B, respectively. Peptide separation was conducted with a linear gradient of 6–43% B in 125 min. The electrospray voltage was 1.8 kV, and the ion transport tube temperature was 320 °C. The isolation width for precursor ions was 1.6 $m/z$, and the fragmentation method was HCD, where the normalized collision energy was 28. After the calibration of the precursor ions' retention times using tryptic peptides of bovine serum albumin (BSA) as references, MS/MS for the precursor ions on the inclusion lists were acquired in scheduled PRM mode with a 10-min retention time window.

The raw LC-PRM data were imported to Skyline version 21.2[25] for processing. The acquired MS/MS of each precursor ion was compared with that in the spectral library, where spectral similarity was gauged using dot product (dotp) value.[26] The presence of 4–6 concurrent fragment ions and a dotp value greater than 0.7 were considered a positive identification. The Skyline data were exported to Excel for further data processing (Table S1c–f). Briefly, the ratio of each peptide derived from RWE protein was calculated using the following normalization procedure: (1) the peak area of the endogenous peptide was divided by that of its corresponding stable isotope-labeled (SIL) peptide or a surrogate standard with a similar retention time; (2) the resulting ratio was further normalized against the ratio of the sum of peak areas for all the light peptides over that for all the heavy peptides in each LC-PRM run. The relative ratios of the peptides were then normalized to that in the Day-0 samples. The peptide ratios in each sample, averaged from the quantification results of two technical replicates, were represented by mean ± SD. The relative ratios of the epitranscriptomic RWE proteins in one biological replicate were calculated by the mean of the relative ratios of the peptides derived from the same protein. The final ratios of the RWE proteins were averaged from the quantification results of two biological replicates (except Day-5 and Day-6, which contained only one replicate). Hierarchical clustering with $Z$-score standardization was performed with Perseus 2.0.3.1.[27] $Z$-score standardization was used to standardize the alterations in protein expression during the differentiation process on the same scale. Proteins were clustered using the Euclidean distance.

## RESULTS AND DISCUSSION

Previous studies showed that osteogenic differentiation of ESCs could be elicited *in vitro* by incubating these cells with $\beta$-glycerophosphate, ascorbic acid, and the active form of

vitamin $D_3$ or dexamethasone.[22,28] We induced osteogenic differentiation of H9 human ESCs by using a previously developed vitamin $D_3$-based monolayer overgrowth culture approach,[23,29] with some minor modifications.[21] Confluent cells prior to differentiation induction were collected as Day-0, and the cells were also collected at 3, 5, 6, 8, 10, 12, 15, and 20 days following differentiation/osteogenesis induction[21] for temporal profiling of epitranscriptomic RWE proteins during osteogenesis (Figure 1). We employed LC-PRM, along with the use of synthetic stable isotope-labeled (SIL) peptides,[30] to examine the relative expression of 154 epitranscriptomic RWE proteins in cells collected at different time points following osteogenic induction (Figure 1). Compared to the discovery approaches, e.g., data-dependent acquisition (DDA) and data-independent acquisition (DIA), PRM-based targeted proteomics provides sensitive and reproducible quantification results for specific proteins of interest, especially those of low abundance. We conducted the experiments in two biological replicates except Day-5 and Day-6, where only one biological replicate was analyzed, owing to inadequate amounts of protein samples available for the other replicate. To obtain reliable quantification results, we analyzed each biological replicate by LC-PRM twice.

In the two biological replicates, we were able to quantify the relative expression levels of 260 and 243 peptides from tryptic digests of the epitranscriptomic RWE proteins. In the first and second replicates, 36 and 34 peptides were quantified based on their corresponding SIL peptides, respectively, and the rest of the peptides were quantified based on surrogate SIL standard peptides with similar retention times. These peptides represented 122 and 121 RWE proteins in the first and second biological replicates, respectively. In this vein, 116 of these protzeins were commonly quantified in the two biological replicates, and they account for approximately 82% of the RWE proteins in the PRM library (Figure S1a). Pearson correlation coefficients between pairs of different time points ranged from 0.2 to 0.8, with 78% of them being lower than 0.7, indicating that the expression profiles of RWE proteins at different time points are distinct from each other (Figure S1b). Violin plots showed that the medians of the relative standard deviation for the samples from different differentiation days are within 30%, indicating the good reproducibility of the results obtained from the two biological replicates (Figure S1c).

To better reveal the temporal changes in the abundances of epitranscriptomic RWE proteins during osteogenic differentiation, we normalized the LC-PRM quantification results to the corresponding results of Day-0 and $Log_2$-transformed the obtained ratios, facilitating the investigation about the implications of epitranscriptomic RWE proteins throughout the entire time course of osteogenic differentiation. Hierarchical clustering analysis allowed for the classification of the 116 RWE proteins commonly detected in the two biological replicates into 2 groups (Figure 2A). The majority of the proteins belong to Group 1, which contains 66 RWE proteins exhibiting decreasing expression levels with differentiation time (Figure 2B). Group 2 encompasses 50 proteins, which were down-regulated slightly with time followed by slight increases and then decreases to similar levels as prior to differentiation. Considering that more than half of the RWE proteins were down-regulated during osteogenesis, we focused our subsequent investigation on these proteins.

Gene ontology (GO) analysis of the down-regulated epitranscriptomic RWE proteins in Group 1, using the database for annotation, visualization and integrated discovery (DAVID),[31,32] showed that these proteins are mainly involved in the biological processes of RNA methylation and pseudouridylation (Figure 2C and Figure S2). For instance, the extracted-ion chromatograms of representative peptides of NSUN2 and PUS1 and their corresponding spiked-in SIL peptides (Figure 3A) revealed diminished levels of these two proteins during osteogenesis. Western blot analysis of these two proteins demonstrated similar decreasing trends as obtained from PRM analysis (Figure 3B,C).

LC-PRM quantification results showed that the expression levels of several detected $m^5C$ methyltransferases, i.e., NOP2, NSUN2, NSUN5, and NSUN6, gradually decreased during osteogenesis, suggesting that $m^5C$ and its writer proteins might modulate osteogenesis (Figure S3). Among these proteins, NOP2 and NSUN5 mediate rRNA methylation, NSUN2 catalyzes $m^5C$ formation in tRNA, mRNA, and non-coding RNAs, whereas NSUN6 catalyzes tRNA methylation.[33–37] These NSUN family members have been found to function in multiple biological processes. For instance, NSUN2-catalyzed tRNA methylation is essential for neural stem cell differentiation.[38] Our LC-PRM results indicated that this protein may also be involved in osteogenic differentiation.

The LC-PRM quantification results also showed that the abundances of the major detected pseudouridine synthases exhibited steady diminutions during the entire time course of osteogenic differentiation (Figure S3). In this regard, RNA pseudouridylation was shown to modulate cell differentiation. For instance, DKC1-catalyzed pseudouridylation of small nucleolar RNAs (snoRNAs) enhanced the expression of OCT4 and SOX2, which are important transcription factors for the pluripotency and self-renewal of stem cells.[39] Additionally, PUS7-mediated pseudouridylation of tRNA-derived fragments was found to regulate downstream translation and control stem cell fate decision.[40] These findings suggest potential roles of pseudouridine synthases in osteogenesis.

We next investigated the interrelationship of the epitranscriptomic RWE proteins during osteogenesis (Figure S4). The hub proteins are ranked in the following order of importance: METTL1, TRMT11, NSUN2, TMRT6, PUS7, TRMT112, TRMT1, WDR4, NAT10, and NSUN6 (Figure S4b). LC-PRM quantification results of these proteins are shown in Figure S4c. These hub proteins with the highest interconnectivity to other nodes in the protein–protein interaction (PPI) network are expected to be functionally the most important. Most hub proteins are associated with RNA methylation. Aside from the aforementioned RNA $m^5C$ methyltransferases, many other methyltransferases are also on the list. For instance, METTL1/WDR4, which are the major components of human $N7$-methylguanosine ($m^7G$) methyltransferase complex, are essential regulators in ESCs, and their loss impaired self-renewal and neural differentiation of mouse ESCs.[41] As the only acetyltransferase in the top 10 hub proteins, NAT10 displays a strong correlation with osteogenic differentiation. In particular, NAT10 could promote osteogenic differentiation of human BMSCs by mediating the formation of $N^4$-acetylcytidine ($ac^4C$) in RUNX2 and gremlin 1 mRNAs.[42,43]

To visualize the relationship between the osteogenesis-related proteins and epitranscriptomic RWE proteins, we obtained the osteogenesis gene set from the harmonizome database.[44]

Based on the GeneRIF biological term annotations,[45] the osteogenesis gene set harbors 107 genes co-occurring with the biological process term of osteogenesis. The results of our enrichment analysis of the PPI network showed that several pseudouridine synthases, i.e., RPUSD3, RPUSD4, DKC1, and PUS7, are highly connected with the proteins mediated by the MAPK cascade, including BMP2, CDC42, IGF1, IL6, TGFB3, and TNF in the MCODE_2 cluster (Figure 4A, Table S2). BMP2 is a potent osteogenesis activator, where inflammatory mediators IL6 and TNF positively and negatively modulate the BMP2-induced osteogenic differentiation in BMSCs, respectively.[41,46] Other proteins associated with mRNA methylation and bone development were included in the MCODE_1 cluster with a high connectivity score. For instance, collagen type I $\alpha$1 and $\alpha$2 (COL1A1 and COL1A2) are highly correlated, directly or indirectly, with RNA-modifying proteins in the MCODE_1 cluster (Figure 4B). COL1A1 and COL1A2 are important components of extracellular matrix in humans and are especially abundant in the bone, skin, and connective tissues.[47] Autosomal dominant mutations in *COL1A1* and *COL1A2* genes are the major causes of OI, where approximately 85–90% of OI patients carry mutations in these two genes.[48] The association between COL1A1/COL1A2 and RNA-modifying proteins suggests that aberrant expression or activities of RNA-modifying proteins may be associated with OI.

Interestingly, 9 out of the 14 epitranscriptomic RWE proteins in MCODE_1 belong to Group 1 (Figure 4C). To further explore the functions of epitranscriptomic RWE proteins in OI, we selected METTL1 (Figure S5), which ranked the top among the hub proteins in Group 1 (Figure S4b), for gene set enrichment analysis (GSEA). Here, we used previously published RNA-seq data of 10 OI patients for the subsequent analysis. We stratified the RNA-seq data for the patients into the groups of high and low mRNA expression of *METTL1* using its median value as a cutoff. The phenotype with high *METTL1* mRNA expression also exhibits high mRNA expression of all genes from RWE-Group 1 and GO_BP RNA methylation gene sets (Figure S6a,b).

Results from the GSEA between stratified RNA-seq data and the hallmark gene sets from MsigDB showed that 34 out of 50 gene sets were up-regulated in phenotype with low expression of *METTL1* mRNA. Among these up-regulated gene sets, 10 were significantly up-regulated with FDR being < 25%. The interferon $\alpha$ and $\gamma$ (IFN-$\alpha$ and IFN-$\gamma$) response gene sets were the most significantly enriched gene sets (Figure S6c,d). IFN-$\alpha$ and IFN-$\gamma$ are cytokines involved in regulating osteoblast differentiation, an important step in osteogenesis, and they are considered as osteoblastogenic cytokines.[49] These findings suggest the role of METTL1 in regulating osteogenesis through the cytokine network.

## CONCLUSIONS

In summary, we conducted temporal profiling of 154 epitranscriptomic RWE proteins during osteogenic differentiation of H9 human ESCs. We were able to quantify the alterations in expression levels of 127 epitranscriptomic RWE proteins throughout the process of osteogenic differentiation in human ESCs. They represent 82% of the RWE proteins in the PRM library, and we found that nearly half of the epitranscriptomic RWE proteins were down-regulated during osteogenic differentiation. GO analysis showed that the down-regulated RWE proteins are mainly associated with RNA methylation and

pseudouridylation. PPI network analysis indicated the significance of METTL1 among the down-regulated RWE proteins and a strong association between down-regulated RWE proteins and bone formation. GSEA results of previously published RNA-seq data from OI patients revealed a potential role of METTL1 during osteogenesis. Together, our results unveiled potential regulatory roles of epitranscriptomic RWE proteins during osteogenic differentiation of human H9 ESCs, and our work offered novel insights into the mechanisms of osteogenesis process and may benefit future development of therapeutic approaches for treating osteo-degenerative diseases.

## Supplementary Material

Refer to Web version on PubMed Central for supplementary material.

## ACKNOWLEDGMENTS

This work was supported by the National Institutes of Health (R01 CA236204 to Y.W. and R01 DE 025330 to N.z.N.).

## Data Availability Statement

The LC–MS/MS raw data and related files were deposited to the ProteomeXchange Consortium via the PRIDE[50] partner repository with the data set identifier PXD039249.

## REFERENCES

(1). Cech DJ; Martin ST Skeletal System Changes. In Functional Movement Development Across the Life Span, 3rd ed.; Cech DJ, Martin ST, Eds.; W.B. Saunders: Saint Louis, 2012; Chapter 6, pp 105–128.

(2). zur Nieden NI Embryonic stem cells for osteo-degenerative diseases. Methods Mol. Biol 2011, 690, 1–30. [PubMed: 21042982]

(3). Shen Y; Huang X; Wu J; Lin X; Zhou X; Zhu Z; Pan X; Xu J; Qiao J; Zhang T; Ye L; Jiang H; Ren Y; Shan P-F The global burden of osteoporosis, low bone mass, and its related fracture in 204 countries and territories, 1990–2019. Front. Endocrinol 2022, 13, 882241.

(4). Tu KN; Lie JD; Wan CKV; Cameron M; Austel AG; Nguyen JK; Van K; Hyun D.Osteoporosis: a review of treatment options. Pharm. Ther 2018, 43, 92–104.

(5). Paul Tuck S; Layfield R; Walker J; Mekkayil B; Francis R.Adult Paget's disease of bone: a review. Rheumatol 2017, 56, 2050–2059.

(6). Drabkin A; Rothman MS; Wassenaar E; Mascolo M; Mehler PS Assessment and clinical management of bone disease in adults with eating disorders: a review. J. Eat. Disord 2017, 5, 42. [PubMed: 29214023]

(7). Zhytnik L; Simm K; Salumets A; Peters M; Märtson A; Maasalu K.Reproductive options for families at risk of Osteogenesis Imperfecta: a review. Orphanet J. Rare Dis 2020, 15, 128. [PubMed: 32460820]

(8). Aly RM Current state of stem cell-based therapies: an overview. Stem Cell Investig 2020, 7, 8.

(9). Hoang DM; Pham PT; Bach TQ; Ngo ATL; Nguyen QT; Phan TTK; Nguyen GH; Le PTT; Hoang VT; Forsyth NR; Heke M; Nguyen LT Stem cell-based therapy for human diseases. Signal Transduct. Targeted Ther 2022, 7, 272.

(10). Ji Y; Hu C; Chen Z; Li Y; Dai J; Zhang J; Shu Q.Clinical trials of stem cell-based therapies for pediatric diseases: a comprehensive analysis of trials registered on ClinicalTrials.gov and the ICTRP portal site. Stem Cell Res. Ther 2022, 13, 307. [PubMed: 35841064]

(11). Jiang Y; Zhang P; Zhang X; Lv L; Zhou Y.Advances in mesenchymal stem cell transplantation for the treatment of osteoporosis. Cell Prolif 2021, 54, No. e12956.

(12). Götherström C; Walther-Jallow L.Stem cell therapy as a treatment for osteogenesis imperfecta. Curr. Osteoporos. Rep 2020, 18, 337–343. [PubMed: 32710427]

(13). Jaishankar A; Barthelery M; Freeman WM; Salli U; Ritty TM; Vrana KE Human embryonic and mesenchymal stem cells express different nuclear proteomes. Stem Cells Dev 2009, 18, 793–802. [PubMed: 18821827]

(14). Liu Y; Zhang X-L; Chen L; Lin X; Xiong D; Xu F; Yuan L-Q; Liao E-Y Epigenetic mechanisms of bone regeneration and homeostasis. Prog. Biophys. Mol. Biol 2016, 122, 85–92. [PubMed: 26797037]

(15). Chen X; Hua W; Huang X; Chen Y; Zhang J; Li G.Regulatory role of RNA N(6)-methyladenosine modification in bone biology and osteoporosis. Front. Endocrinol 2020, 10, 911.

(16). Roundtree IA; Evans ME; Pan T; He C.Dynamic RNA modifications in gene expression regulation. Cell 2017, 169, 1187–1200. [PubMed: 28622506]

(17). Boccaletto P; Stefaniak F; Ray A; Cappannini A; Mukherjee S; Purta E; Kurkowska M; Shirvanizadeh N; Destefanis E; Groza P; Avsar G; Romitelli A; Pir P; Dassi E; Conticello SG; Aguilo F; Bujnicki JM MODOMICS: a database of RNA modification pathways. 2021 update. Nucleic Acids Res. 2022, 50, D231–D235. [PubMed: 34893873]

(18). Liu T; Zheng X; Wang C; Wang C; Jiang S; Li B; Chen P; Xu W; Zheng H; Yang R; Huang X; Zhang X; Jiang L.The m6A “reader” YTHDF1 promotes osteogenesis of bone marrow mesenchymal stem cells through translational control of ZNF839. Cell Death Dis 2021, 12, 1078. [PubMed: 34772913]

(19). Tian C; Huang Y; Li Q; Feng Z; Xu Q.Mettl3 regulates osteogenic differentiation and alternative splicing of vegfa in bone marrow mesenchymal stem cells. Int. J. Mol. Sci 2019, 20, 551. [PubMed: 30696066]

(20). Shen G-S; Zhou H-B; Zhang H; Chen B; Liu Z-P; Yuan Y; Zhou X-Z; Xu Y-J The GDF11-FTO-PPAR$\gamma$ axis controls the shift of osteoporotic MSC fate to adipocyte and inhibits bone formation during osteoporosis. Biochim. Biophys. Acta 2018, 1864, 3644–3654.

(21). Yang Y-Y; Soh R; Vera-Colón M; Huang M; zur Nieden NI; Wang Y.Targeted Proteomic Profiling Revealed Roles of Small GTPases during Osteogenic Differentiation. Anal. Chem 2023, 95, 6879–6887. [PubMed: 37083350]

(22). zur Nieden NI; Kempka G; Ahr HJ In vitro differentiation of embryonic stem cells into mineralized osteoblasts. Differentiation 2003, 71, 18–27. [PubMed: 12558600]

(23). Kuske B; Savkovic V; zur Nieden NI Improved media compositions for the differentiation of embryonic stem cells into osteoblasts and chondrocytes. In Embryonic Stem Cell Therapy for Osteo-Degenerative Diseases; Springer: 2011; pp 195–215.

(24). Sparks N; Williams D; zur Nieden NI Transcriptome analysis reveals toxicant-induced miRNA signatures associated with aberrant human embryonic stem cell osteoblast differentiation. Birth Defects Res 2021, 113, 784.

(25). MacLean B; Tomazela DM; Shulman N; Chambers M; Finney GL; Frewen B; Kern R; Tabb DL; Liebler DC; MacCoss MJ Skyline: an open source document editor for creating and analyzing targeted proteomics experiments. Bioinformatics 2010, 26, 966–968. [PubMed: 20147306]

(26). Kawahara R; Bollinger JG; Rivera C; Ribeiro ACP; Brandão TB; Leme AFP; MacCoss MJ A targeted proteomic strategy for the measurement of oral cancer candidate biomarkers in human saliva. Proteomics 2016, 16, 159–173. [PubMed: 26552850]

(27). Tyanova S; Temu T; Sinitcyn P; Carlson A; Hein MY; Geiger T; Mann M; Cox J.The Perseus computational platform for comprehensive analysis of (prote)omics data. Nature Methods 2016, 13, 731–740. [PubMed: 27348712]

(28). Duplomb L; Dagouassat M; Jourdon P; Heymann D.Concise review: embryonic stem cells: a new tool to study osteoblast and osteoclast differentiation. Stem Cells 2007, 25, 544–552. [PubMed: 17095705]

(29). Karp JM; Ferreira LS; Khademhosseini A; Kwon AH; Yeh J; Langer RS Cultivation of human embryonic stem cells without the embryoid body step enhances osteogenesis in vitro. Stem Cells 2006, 24, 835–843. [PubMed: 16253980]

(30). Qi TF; Liu X; Tang F; Yin J; Yu K; Wang Y.Targeted quantitative profiling of epitranscriptomic reader, writer, and eraser proteins using stable isotope-labeled peptides. Anal. Chem 2022, 94, 12559–12564. [PubMed: 36084281]

(31). Sherman BT; Hao M; Qiu J; Jiao X; Baseler MW; Lane HC; Imamichi T; Chang W.DAVID: a web server for functional enrichment analysis and functional annotation of gene lists (2021 update). Nucleic Acids Res. 2022, 50, W216–W221. [PubMed: 35325185]

(32). Huang DW; Sherman BT; Lempicki RA Systematic and integrative analysis of large gene lists using DAVID bioinformatics resources. Nature Protocols 2009, 4, 44–57. [PubMed: 19131956]

(33). Bourgeois G; Ney M; Gaspar I; Aigueperse C; Schaefer M; Kellner S; Helm M; Motorin Y.Eukaryotic rRNA Modification by Yeast 5-Methylcytosine-Methyltransferases and Human Proliferation-Associated Antigen p120. PLOS ONE 2015, 10, No. e0133321.

(34). Cámara Y; Asin-Cayuela J; Park CB; Metodiev MD; Shi Y; Ruzzenente B; Kukat C; Habermann B; Wibom R; Hultenby K; Franz T; Erdjument-Bromage H; Tempst P; Hallberg BM; Gustafsson CM; Larsson N-G MTERF4 Regulates Translation by Targeting the Methyltransferase NSUN4 to the Mammalian Mitochondrial Ribosome. Cell Metabolism 2011, 13, 527–539. [PubMed: 21531335]

(35). Heissenberger C; Liendl L; Nagelreiter F; Gonskikh Y; Yang G; Stelzer EM; Krammer TL; Micutkova L; Vogt S; Kreil DP; Sekot G; Siena E; Poser I; Harreither E; Linder A; Ehret V; Helbich TH; Grillari-Voglauer R; Jansen-Dürr P; Koš M; Polacek N; Grillari J; Schosserer M.Loss of the ribosomal RNA methyltransferase NSUN5 impairs global protein synthesis and normal growth. Nucleic Acids Res. 2019, 47, 11807–11825. [PubMed: 31722427]

(36). Haag S; Warda AS; Kretschmer J; Günnigmann, M. A.; Höbartner, C.; Bohnsack, M. T. NSUN6 is a human RNA methyltransferase that catalyzes formation of m5C72 in specific tRNAs. RNA 2015, 21, 1532–1543. [PubMed: 26160102]

(37). Bohnsack KE; Höbartner C; Bohnsack MT Eukaryotic 5-methylcytosine (m5C) RNA Methyltransferases: Mechanisms, Cellular Functions, and Links to Disease. Genes 2019, 10, 102. [PubMed: 30704115]

(38). Flores JV; Cordero-Espinoza L; Oeztuerk-Winder F; Andersson-Rolf A; Selmi T; Blanco S; Tailor J; Dietmann S; Frye M.Cytosine-5 RNA methylation regulates neural stem cell differentiation and motility. Stem Cell Reports 2017, 8, 112–124. [PubMed: 28041877]

(39). Fong YW; Ho JJ; Inouye C; Tjian R.The dyskerin ribonucleoprotein complex as an OCT4/SOX2 coactivator in embryonic stem cells. eLife 2014, 3, No. e03573.

(40). Guzzi N; Cieśla M; Ngoc PCT; Lang S; Arora S; Dimitriou M; Pimková K; Sommarin MNE; Munita R; Lubas M; Lim Y; Okuyama K; Soneji S; Karlsson G; Hansson J; Jönsson G; Lund AH; Sigvardsson M; Hellström-Lindberg E; Hsieh AC; Bellodi C.Pseudouridylation of tRNA-derived fragments steers translational control in stem cells. Cell 2018, 173, 1204–1216. [PubMed: 29628141]

(41). Huang R-L; Sun Y; Ho C-K; Liu K; Tang Q-Q; Xie Y; Li Q.IL-6 potentiates BMP-2-induced osteogenesis and adipogenesis via two different BMPR1A-mediated pathways. Cell Death Dis 2018, 9, 144. [PubMed: 29396550]

(42). Yang W; Li HY; Wu YF; Mi RJ; Liu WZ; Shen X; Lu YX; Jiang YH; Ma MJ; Shen HY ac4C acetylation of RUNX2 catalyzed by NAT10 spurs osteogenesis of BMSCs and prevents ovariectomy-induced bone loss. Molecular Therapy - Nucleic Acids 2021, 26, 135–147. [PubMed: 34513300]

(43). Zhu Z; Xing X; Huang S; Tu Y.NAT10 promotes osteogenic differentiation of mesenchymal stem cells by mediating N4-acetylcytidine modification of gremlin 1. Stem Cells International 2021, 2021, 8833527.

(44). Rouillard AD; Gundersen GW; Fernandez NF; Wang Z; Monteiro CD; McDermott MG; Ma'ayan A.The harmonizome: a collection of processed datasets gathered to serve and mine knowledge about genes and proteins. Database 2016, 2016, baw100.

(45). Mitchell JA; Aronson AR; Mork JG; Folk LC; Humphrey SM; Ward JM Gene indexing: characterization and analysis of NLM's GeneRIFs. AMIA Annu. Symp. Proc 2003, 2003, 460–464. [PubMed: 14728215]

(46). Huang RL; Yuan Y; Tu J; Zou GM; Li Q.Opposing TNF-$\alpha$/IL-1$\beta$- and BMP-2-activated MAPK signaling pathways converge on Runx2 to regulate BMP-2-induced osteoblastic differentiation. Cell Death Dis 2014, 5, e1187–e1187. [PubMed: 24743742]

(47). Henriksen K; Karsdal MA Type I collagen. In Biochemistry of Collagens, Laminins and Elastin, 2nd ed.; Karsdal MA, Ed.; Academic Press: 2019; Chapter 1, pp 1–12.

(48). Forlino A; Marini JC Osteogenesis imperfecta. The Lancet 2016, 387, 1657–1671.

(49). Amarasekara DS; Kim S; Rho J.Regulation of osteoblast differentiation by cytokine networks. Int. J. Mol. Sci 2021, 22, 2851. [PubMed: 33799644]

(50). Perez-Riverol Y; Bai J; Bandla C; García-Seisdedos D; Hewapathirana S; Kamatchinathan S; Kundu DJ; Prakash A; Frericks-Zipper A; Eisenacher M; Walzer M; Wang S; Brazma A; Vizcaíno, Juan A. The PRIDE database resources in 2022: a hub for mass spectrometry-based proteomics evidences. Nucleic Acids Res. 2022, 50, D543–D552. [PubMed: 34723319]

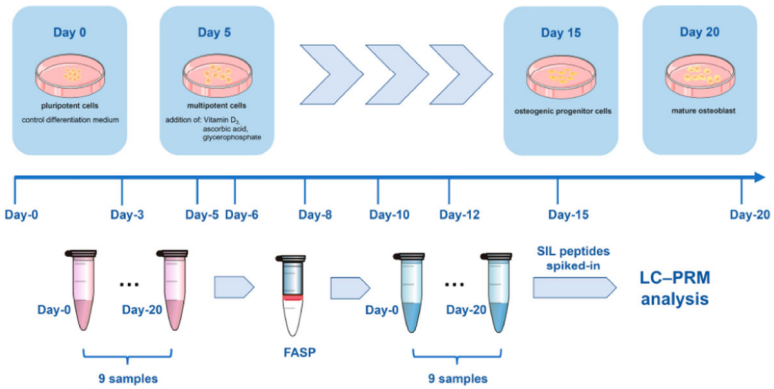


**Figure 1.**

LC-parallel-reaction monitoring (PRM) workflow for examining the alterations in expression of epitranscriptomic RWE proteins during osteogenic differentiation of H9 human ESCs. H9 human ESCs were first incubated in control differentiation medium for 5 days, switched to a medium containing osteogenic differentiation cocktail, and incubated for 15 additional days. Confluent cells prior to differentiation induction (Day-0) and cells at different time points following differentiation/osteogenesis induction were collected and processed with the filter-aided sample preparation (FASP) protocol. Temporal profiling of epitranscriptomic RWE proteins during osteogenesis was performed by using LC-PRM with SIL peptides as internal or surrogate standards.

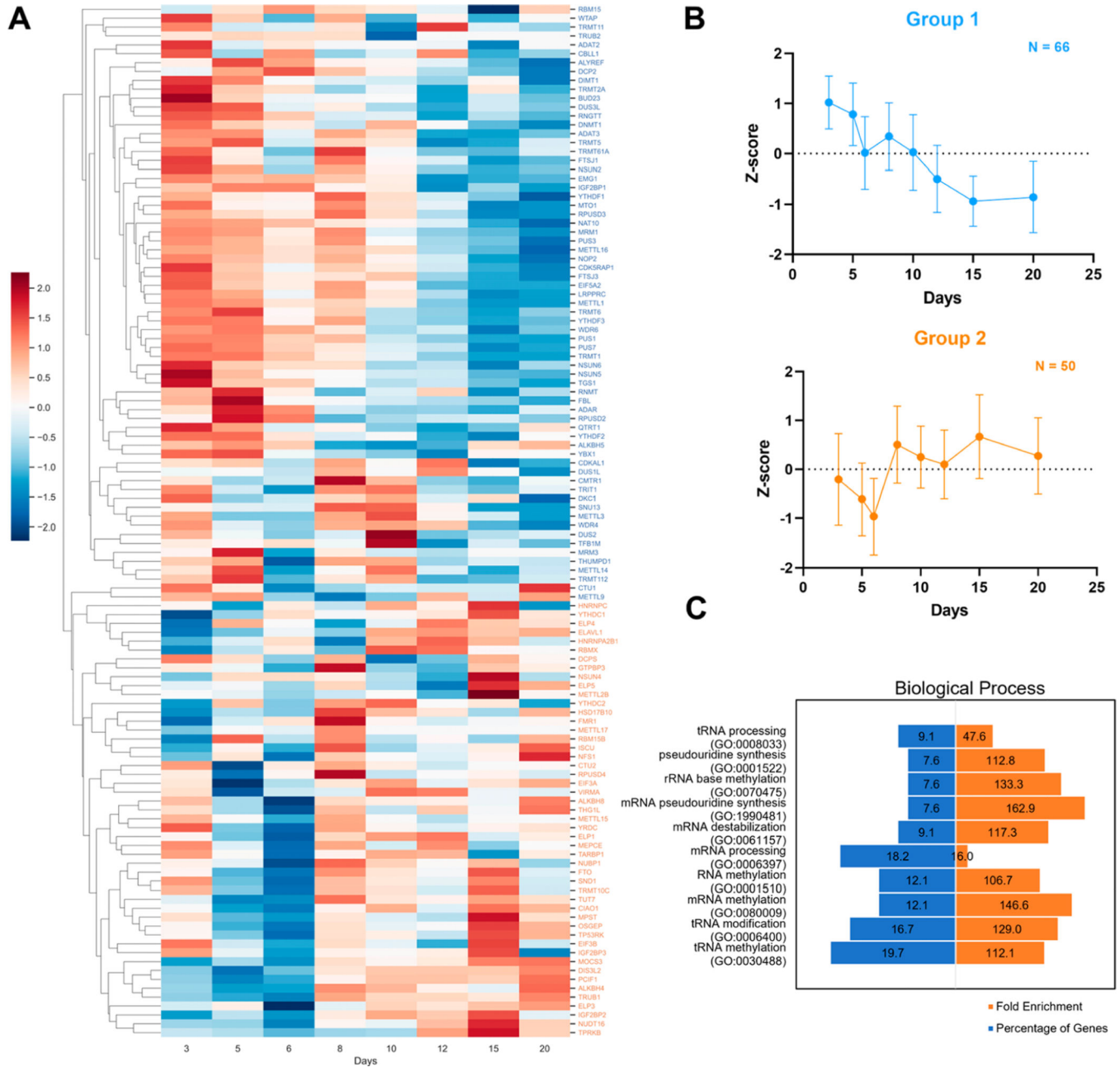


**Figure 2.**

Hierarchical clustering analysis of the quantified epitranscriptomic RWE proteins with cluster-specific *Z*-score trends and gene ontology (GO) analysis. (A) Hierarchical clustering with *Z*-score standardization of $Log_2$-transformed expression fold changes of the 126 epitranscriptomic RWE proteins at different time points relative to Day-0. The expression fold differences were averaged from two biological replicates, except Day-5 and Day-6, which included only one replicate due to a lack of sufficient protein samples. Hierarchical clustering was performed using Perseus 2.0.3.1, where red and blue boxes designate up- and down-regulated proteins, respectively, during the osteogenic differentiation of H9 human ESCs. Proteins were clustered using Euclidean distance. (B) *Z*-score plots depicting the

changing trends of proteins in different clusters. The data represent the mean ± SD of results from the proteins in different clusters, where the number of proteins in each cluster is indicated. (C) GO analysis of the down-regulated epitranscriptomic RWE proteins in Group 1 using DAVID functional annotation. Top 10 annotated terms under biological processes are listed. The percentage of the genes and enrichment fold are represented as blue and orange bars, respectively.

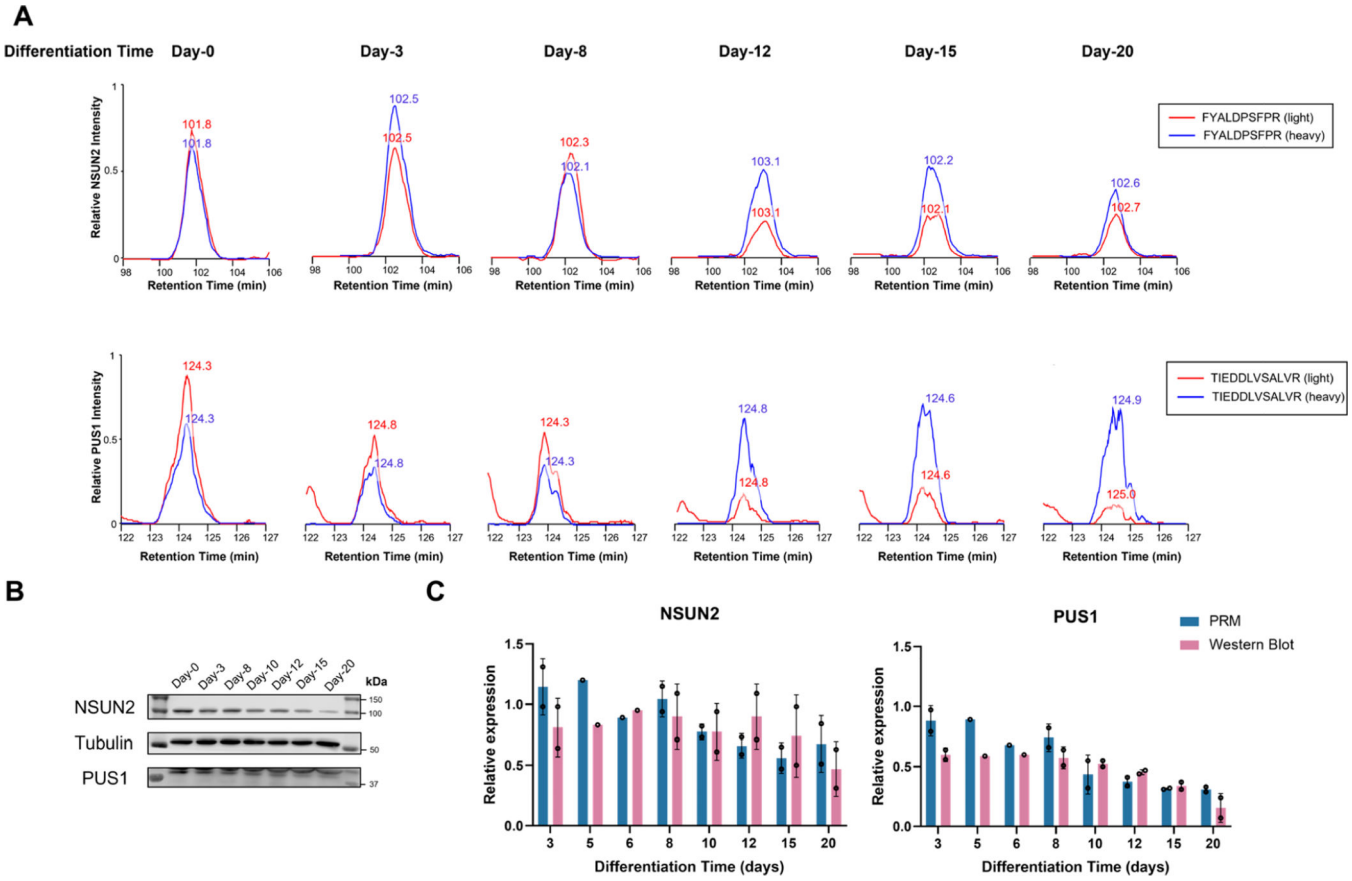


**Figure 3.**

Western blot validation of the LC-PRM quantification results of NSUN2 and PUS1. (A) Extracted-ion chromatograms of tryptic peptides FYALDPSFPR (from NSUN2) and TIEDDLVSALVR (from PUS1), and their corresponding SIL peptides. (B) Western blot results of NSUN2 and PUS1. (C) Comparison of the LC-PRM results with Western blot results for NSUN2 and PUS1. Relative expression of the proteins on different days following osteogenic induction was compared with the results of Day-0. The data represent mean ± SD of results from two independent experiments except Day-5 and Day-6.

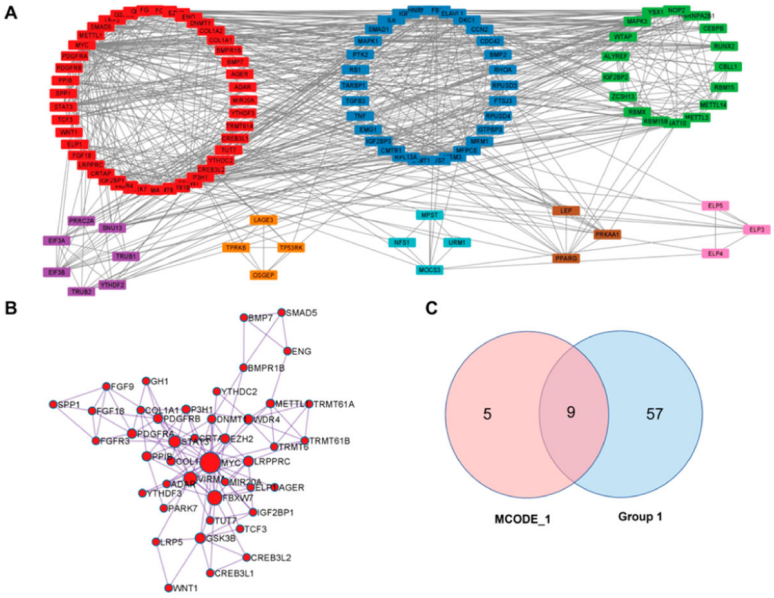


**Figure 4.**

PPI network analysis of osteogenesis-related proteins and epitranscriptomic RWE proteins. (A) PPI network of osteogenesis-related proteins and epitranscriptomic RWE proteins detected in this study using the STRING database, processed with MCODE analysis via Metascape. Eight MCODE complexes were identified and ranked according to their interconnectivity. (B) PPI network of the MCODE_1 complex. (C) Venn diagram comparing the numbers of RWE proteins in MCODE_1 and Group 1.